Available online at www.sciencedirect.com
ScienceDirect
Journal of Computational Physics 225 (2007) 509–527
JOURNAL OF COMPUTATIONAL PHYSICS
www.elsevier.com/locate/jcp

Calculating the free energy of nearly jammed hard-particle packings using molecular dynamics

Aleksandar Donev [a,b], Frank H. Stillinger [c], Salvatore Torquato [a,b,c,d,*]

[a] *Program in Applied and Computational Mathematics, Princeton University, Princeton, NJ 08544, USA*
[b] *Princeton Institute for the Science and Technology of Materials, Princeton University, Princeton, NJ 08544, USA*
[c] *Department of Chemistry, Princeton University, Princeton, NJ 08544, USA*
[d] *Princeton Center for Theoretical Physics, Princeton University, Princeton, NJ 08544, USA*

Received 30 July 2006; received in revised form 22 November 2006; accepted 15 December 2006
Available online 10 January 2007

Abstract

We present a new event-driven molecular dynamics (MD) algorithm for measuring the free energy of nearly jammed packings of spherical and non-spherical hard particles. This Bounding Cell Molecular Dynamics (BCMD) algorithm exactly calculates the free-energy of a single-occupancy cell (SOC) model in which each particle is restricted to a neighborhood of its initial position using a hard-wall bounding cell. Our MD algorithm generalizes previous ones in the literature by enabling us to study non-spherical particles as well as to measure the free-energy change during continuous irreversible transformations. Moreover, we make connections to the well-studied problem of computing the volume of convex bodies in high dimensions using random walks. We test and verify the numerical accuracy of the method by comparing against rigorous asymptotic results for the free energy of jammed and isostatic disordered packings of both hard spheres and ellipsoids, for which the free energy can be calculated directly as the volume of a high-dimensional simplex. We also compare our results to previously published Monte Carlo results for hard-sphere crystals near melting and jamming and find excellent agreement. We have successfully used the BCMD algorithm to determine the configurational and free-volume contributions to the free energy of glassy states of binary hard disks [A. Donev, F.H. Stillinger, S. Torquato, Do binary hard disks exhibit an ideal glass transition? Phys. Rev. Lett. 96 (22) (2006) 225502]. The algorithm can also be used to determine phases with locally- or globally-minimal free energy, to calculate the free-energy cost of point and extended crystal defects, or to calculate the elastic moduli of glassy or crystalline solids, among other potential applications.

Keywords: Free energy; Molecular dynamics; Jamming; Hard particles

* Corresponding author. Address: Department of Chemistry, Princeton University, Princeton, NJ 08544, USA. Tel.: +1 609 258 3341; fax: +1 609 258 6746.
E-mail address: torquato@electron.princeton.edu (S. Torquato).

0021-9991/$ - see front matter © 2007 Elsevier Inc. All rights reserved.
doi:10.1016/j.jcp.2006.12.013

1. Introduction

Calculating the free energy of atomic and molecular systems is a fundamental problem in computational physics [1]. The thermodynamically stable phase under certain macroscopic conditions is the one with the minimal free energy, and identification of the stable phases and the transitions between them requires free-energy calculations. The determination of the thermodynamically stable solid phase of the hard-sphere system [2–4] and the determination of the configurational entropy of supercooled liquids [5–8] is a challenging problem. The latter problem in particular is of significant importance, since it provides insight into the validity of ideal-glass transition hypotheses, thus addressing one of the most fundamental open problems in the study of glasses.

Hard-particle systems are an excellent testbed for such studies because of the balance they offer between a simple model and resulting complex behavior. They have been shown to exhibit a variety of phases, including liquid, solid, liquid crystal and glassy states of matter. Furthermore, they can be simulated with very fast specialized simulation techniques. Calculating the free energy of structured phases such as solid, glassy and liquid crystal phases is a particular challenge, and various approaches have been developed, mostly using Monte Carlo (MC) algorithms [1]. Hard-particle systems are, however, best simulated using event-driven Molecular Dynamics (MD) algorithms [9]. In this paper, we present in detail an algorithm for computing the free energy (equivalently, entropy) of nearly jammed hard particle packings, i.e., hard-particle systems where diffusion can be ignored and particles remain localized in the vicinity of their initial configuration for long times. Note that (nearly) jammed packings are not in thermodynamic equilibrium and therefore the free energy we calculate is not the equilibrium free energy at the given packing fraction (density), but rather, it is the *free-volume contribution* to the thermodynamic free energy. We have successfully applied the algorithm to disordered (glassy) jammed hard-sphere packings and demonstrated that previous claims of an ideal-glass transition in binary hard-sphere systems need to re-evaluated [10,11].

The algorithm that we develop here is a direct extension of the collision-driven MD algorithm that we developed in detail in Ref. [9], and, in fact, Ref. [9] provides most of the details necessary to implement it. Our Bounding Cell MD (BCMD) algorithm is based on the tether method of Speedy [12] and calculates the free-energy of a single-occupancy cell (SOC) model [2] in which each particle is restricted to a neighborhood of its initial position using a hard-wall bounding cell. The BCMD algorithm can be applied to non-spherical particles, and it can measure the free-energy change during continuous irreversible transformations, in contrast to previous MD algorithms. We test and verify the numerical accuracy of the method by comparing it against rigorous asymptotic results for the free energy of jammed and isostatic disordered packings of both hard spheres and ellipsoids, for which the free energy can be calculated directly as the volume of a high-dimensional simplex. Previous algorithms have only been verified by comparing to earlier results obtained with similar methods, or other indirect methods. Here we report the first free-energy calculations for a non-trivial hard-particle system employing a deterministic method. We also compare our results to previously published Monte Carlo results for hard-sphere crystals and find excellent agreement. In the appendix, we discuss the connections of our algorithm with the best-known algorithms for computing the volume of convex bodies in high dimensions, as well as the effects of boundary conditions.

In Section 2, we provide a brief mathematical introduction to the problem, focusing on the jamming limit for hard-particle packings. We then describe the BCMD algorithm in Section 3 in considerable detail, and give an illustrative example in Section 4.1. We apply the algorithm to hard-sphere crystals as well as isostatic jammed packings of spheres and ellipses in Section 4, and verify its high numerical accuracy. Several technical details are further developed in the appendices.

2. Background

The background and notation for this paper have been presented in greater detail in Refs. [13,9] and references therein. Here we only briefly review some of this material.

We consider a thermal system of hard particles with covering fraction (or density) ϕ, characterized by the particle displacements $\Delta\mathbf{Q} = (\Delta\mathbf{q}_1, \ldots, \Delta\mathbf{q}_N)$ from an ideal *collectively jammed* [14] configuration $\mathbf{Q}_J$ with jam-

ming density ϕ_J. Roughly speaking, a collectively jammed (compactly packed, mechanically stable) packing is one where the non-overlap conditions preclude all collective particle motions [14], i.e., the particles are locked in their positions despite thermal agitation (shaking). For spheres, $\Delta\mathbf{q} \equiv \Delta\mathbf{r}$ consists of only the centroid displacement. For non-spherical particles, $\Delta\mathbf{q} = (\Delta\mathbf{r}, \Delta\boldsymbol{\varphi})$ also includes the angular displacement, which here we represent as a directed angle or rotation, i.e., the direction of $\Delta\boldsymbol{\varphi}$ gives the axis of rotation and its magnitude the angle of rotation. For simplicity we will focus here on sphere packings and denote the configuration with $\mathbf{R}$ unless we explicitly indicate the non-spherical particles, in which case we will revert to $\mathbf{Q}$. Let d_f be the number of degrees of freedom per particle, so that $\Delta\mathbf{Q}$ is a point in Nd_f-dimensional configuration space. Depending on the boundary conditions, certain additional constraints, such as freezing the center of mass, may be imposed, reducing the number of degrees of freedom to N_f. Note that in more general contexts, $\mathbf{Q}$ may include additional degrees of freedom, e.g. the lattice vectors defining the periodic unit cell.

We are concerned here with *nearly jammed* packings. One can think of having shrunk the particles from the terminal jamming point $(\mathbf{R}_J, \phi_J)$ by a scaling factor

$$\mu = (1-\delta) = (1+\Delta\mu)^{-1}$$

to a reduced density $\phi = \phi_J(1-\delta)^d \approx \phi_J(1-d\delta)$, where $\delta \approx \Delta\mu$ is a small *jamming gap*. It can be shown that, for finite N, there is a sufficiently small δ that does not destroy the jamming property, in the sense that the configuration point $\mathbf{R} = \mathbf{R}_J + \Delta\mathbf{R}$ remains trapped in a small neighborhood $\mathscr{J}_{\Delta\mathbf{R}}$ around $\mathbf{R}_J$ [15]. For the purposes of this work, it is not necessary that the packing be rigorously trapped inside $\mathscr{J}_{\Delta\mathbf{R}}$. Instead, we can consider $\mathscr{J}_{\Delta\mathbf{R}}$ to be the region of configuration space explored by the packing on the time-scale of the observation, i.e., the region of configuration space which makes an appreciable impact on the *measured* thermodynamic properties of the system. Let the number of particle pairs that participate in trapping the configuration inside $\mathscr{J}_{\Delta\mathbf{R}}$ be M. In other words, $\mathscr{J}_{\Delta\mathbf{R}}$ is bounded by M surfaces determining the impenetrability condition between nearby particles. In the jamming limit, M becomes the number of true particle contacts.

Two fundamental assumptions are that $\mathscr{J}_{\Delta\mathbf{R}}$ is bounded (i.e., the displacements of the particles from the jammed point are finite), and that $\mathscr{J}_{\Delta\mathbf{R}}$ is explored ergodically on the time-scale of the measurement of thermodynamic properties, such as pressure. In particular the second assumption enables us to separate the configurational from kinetic portions of phase space. These assumptions allow us to consider both non-equilibrium metastable systems, such as disordered packings, and equilibrium ones, such as perfect crystals. Even in the equilibrium crystal there are occasional very large density fluctuations and therefore particle displacements, and additionally, there are diffusing defects such as vacancies and dislocations. However, at sufficiently high densities, the thermodynamic properties are primarily determined by the configurations close to the perfect crystal. For metastable systems sufficiently long time-scales will eventually lead to large particle rearrangements into the equilibrium configuration. However, such systems can be observed in metastable disordered packing configurations for sufficiently long times as to make meaningful measurements. The techniques presented in this work can be adapted to any system where diffusion can be neglected. Free energy is a concept that strictly speaking applies only to systems in thermodynamic equilibrium, and the free energy we compute is in fact only the free-volume contribution to the thermodynamic free energy of the system. However, phrases such as "free energy of the FCC/HCP lattice" or "free energy of a glass" are used commonly. One can formally make the concept of free energy well-defined for non-equilibrium states by restricting the partition function to configurations in the vicinity of a reference jammed packing; we will do this by use of a cell model in Section 3.

The fundamental problem considered here is computing the logarithm of the volume of the body $\mathscr{V} = |\mathscr{J}_{\Delta\mathbf{R}}|$ in configuration space. In a slight abuse of (equilibrium) thermodynamic nomenclature, we will refer to this as the (non-normalized) free-energy

$$F = -\ln|\mathscr{J}_{\Delta\mathbf{R}}| = Nf,$$

where f is the sought-after free-energy per particle, presumed to be independent of N for sufficiently large systems. Note that, since the internal energy for hard-particle systems identically vanishes, we can fix $k_B T = 1$ and therefore the free energy is simply the negative of the entropy.

2.1. Jamming polytope $\mathscr{P}_{\Delta\mathbf{R}}$: spheres

An interesting problem concerns the shape of $\mathscr{J}_{\Delta\mathbf{R}}$ in the jamming limit $\delta \to 0$. For hard spheres, the answer is well-known: it can be shown that asymptotically the set of displacements that are accessible to the packing approaches a convex *limiting polytope* (a closed polyhedron in arbitrary dimension) $\mathscr{P}_{\Delta\mathbf{R}} \subseteq \mathscr{J}_{\Delta\mathbf{R}}$ [16,17]. This polytope is determined from the linearized impenetrability equations

$$\mathbf{A}^{\mathrm{T}}\Delta\mathbf{R} \leqslant \Delta\mathbf{l}, \tag{1}$$

where $\mathbf{A}$ is the (dimensionless) *rigidity matrix* of the packing, and $\Delta\mathbf{l}$ is the set of interparticle gaps [13,14]. If we use the jamming point as the reference point from which particles are shrunk by δ, then all gaps are equal, $\Delta\mathbf{l} = \delta\mathbf{e}$, where $\mathbf{e}$ is a vector of M elements all equal to one, and we have assumed that all of the spheres have diameter $D = 1$. Therefore, in studying the jamming limit, we can focus on the normalized *jamming polytope* $\mathscr{P}_{\mathbf{x}} : \mathbf{A}^{\mathrm{T}}\mathbf{x} \leqslant \mathbf{e}$, which can be scaled by a factor of δ along all coordinate directions in order to obtain $\mathscr{P}_{\Delta\mathbf{R}}$. In particular, the volume scales in a predictable manner, $|\mathscr{P}_{\Delta\mathbf{R}}| = \delta^{N_{\mathrm{f}}}|\mathscr{P}_{\mathbf{x}}|$. The free energy thus diverges in the well-known free-volume logarithmic fashion [16],

$$f = -d_{\mathrm{f}} \ln \delta - \frac{\ln |\mathscr{P}_{\mathbf{x}}|}{N} = -d_{\mathrm{f}} \ln \delta - f_{\mathrm{J}}, \tag{2}$$

where the fundamental constant f_{J} is determined by the geometry of the jammed state. Computing f_{J} reduces to the well-known #P-hard problem[1] of computing the volume of a polyhedron in high-dimensional spaces. In general, this problem is very difficult and solving it takes exponentially long in the number of dimensions [18]. Our attempts to use state-of-the-art software for computing the volume of polyhedra in high dimensions [19] have failed even for relatively small system sizes due to computational limitations.

An especially tractable case arises when the jammed configuration is *isostatic*, in the sense that $M = N_{\mathrm{f}} + 1$, i.e., in this particular case, the jamming polytope is a *simplex*, whose volume can be computed exactly easily. We have derived [20] a formula for computing the volume directly from the rigidity matrix. Specifically,

$$|\mathscr{P}_{\mathbf{x}}|^{-1} = N_{\mathrm{f}}!|\widetilde{\mathbf{A}}| \prod_{ij} \vec{f}_{ij}, \tag{3}$$

can be calculated using common (sparse) linear-algebra operations. Here the augmented rigidity matrix

$$\widetilde{\mathbf{A}} = \begin{bmatrix} \mathbf{A} \\ \mathbf{e} \end{bmatrix} \tag{4}$$

is invertible, and the vector

$$\vec{\mathbf{f}} = \widetilde{\mathbf{A}}^{-1} \begin{bmatrix} \mathbf{0} \\ 1 \end{bmatrix} \geqslant \mathbf{0}$$

has the physical interpretation of normalized interparticle forces appearing in the force-chains near the jamming point [13]. The normalization is such that the forces sum to one. Ref. [20] analyzes the behavior of Eq. (3) in the thermodynamic limit and its connection to free-energy expressions for systems of soft-spheres.

In Ref. [13] we demonstrated that monodisperse disordered jammed sphere packings in three dimensions are isostatic. Therefore, at least for these packings we have a direct way of computing the free energy in the jamming limit by simply computing the volume of the high-dimensional simplex $\mathscr{P}_{\mathbf{x}}$. We will use this to test the numerical accuracy of our molecular dynamics method for measuring the free energy.

2.2. Jamming polytope $\mathscr{P}_{\Delta\mathbf{Q}}$: non-spherical particles

Complications to this simple and intuitive jamming polytope picture arise for non-spherical particles. In particular, $\mathscr{J}_{\Delta\mathbf{Q}}$ does not necessarily approach a polytope in the jamming limit, but rather, it can have some

[1] The complexity class #P is the set of counting problems associated with the decision problems in the set of NP-hard problems.

curved (quadratic) surfaces which cannot be linearized no matter how close to the jamming point. In particular, we have shown that nearly jammed disordered ellipsoid packings can be very hypostatic, i.e., $M < N_f + 1$ [21]. No closed polytope can have fewer faces than a simplex, so it is clear that such packings do not fit the polytope picture. In such packings, we have found evidence of dynamics with multiple time-scales which is not ergodic on typical simulation time-scales. Due to this additional layer of complexity, we will not try to study such jammed hypostatic ellipsoid packings in this work. Instead, we will produce packings of ellipses for which the polytope picture does apply, and the relevant simplex is the polytope $\mathscr{P}_{\Delta\mathbf{Q}}$ given by

$$\mathbf{A}^T\Delta\mathbf{Q} \leqslant \Delta\mathbf{l}, \tag{5}$$

where $\mathbf{A}$ is a generalized rigidity matrix. Such packings are jammed to first-order (first-order rigid [22]). The only modification of the sphere-packing machinery necessary is to append additional rows to $\mathbf{A}$ corresponding to the rotational degrees of freedom. The rigidity matrix $\mathbf{A}$ has non-zero entries in the rows corresponding to the d_f degrees of freedom of a given particle only in the columns corresponding to contacts of that particle. For spheres, that block of d_f entries is equal to the (unit) normal vector $\mathbf{n}$ at the point of contact [14]. For ellipsoids, this block gets replaced with

$$\begin{bmatrix} \mathbf{n} \\ \mathbf{r}_C \times \mathbf{n} \end{bmatrix},$$

where $\mathbf{r}_C$ is the point of contact relative to the particle centroid. Additionally, $\Delta\mathbf{l} = \delta\tilde{\mathbf{e}}$, where $\tilde{\mathbf{e}}$ is still of order unity but the exact values depend on the geometry of the contacts instead of all being unity. Alternatively, one can scale the columns of the rigidity matrix appropriately in order to get $\delta\mathbf{e}$ on the right hand side of Eq. (5). Since the translational degrees of freedom have a length scale while the rotational do not, we renormalize all distances so that the linear extents of each particle are dimensionless, e.g. the smallest semiaxis of an ellipsoid is unity.[2]

3. Molecular dynamic method for measuring f

Traditional molecular simulation methods can only measure the difference in free energy between two states, typically by constructing a reversible path between the two states, one of which has known free energy [1]. The problem is usually in finding a state for which the free-energy is known analytically, and which can be connected to the state of interest by a reversible path free of (first-order) phase transitions. The classical molecular dynamics (MD) method for hard-sphere crystals is to use the so-called *single-occupancy cell* (SOC) model, in which space is partitioned into N cells, typically the Voronoi polyhedra of each sphere, and the centroid of each particle is constrained to remain fully within its (polyhedral) cell [2]. In the high density limit, the system is (virtually) indistinguishable from the unconstrained crystal, and in the low-density limit the system is an SOC ideal gas, in which the free-energy can be calculated easily. The classical Monte Carlo (MC) method, on the other hand, uses a crystal state in which the particles are constrained to remain within a small neighborhood of the equilibrium crystal sites by virtue of strong harmonic springs (the so-called Einstein crystal) [23]. In the limit of very stiff springs, the hard-particle interactions become negligible and the free-energy can be calculated exactly. Both of these methods have major disadvantages. The MD method requires a complicated polyhedral cell complex, which would be rather non-trivial to construct for non-crystal packings or for systems of non-spherical particles. The MC method on the other hand requires introducing "soft" (spring) interactions into an otherwise hard-particle problem, so that special efficient hard-particle techniques such as event-driven MD cannot be substituted for MC. Additionally, both methods have an approximate (extrapolated) termination criterion, one in a limit of zero density, the other in the limit of sufficiently strong interactions.

The MD method developed here essentially combines the two methods to obtain a method which uses only hard-particle interactions and is also readily applicable to disordered configurations and to non-spherical

[2] A more consistent choice would have been to follow the sphere example and make the smallest axis (diameter) unity. However, the usual overlap (or distance) function used for spheres differs by a factor of 2 (near jamming) from that used for ellipsoids [9].

particles. Additionally, it has a well-defined termination criterion. It is based on the *tether-method* that Speedy introduced for spheres [12], however, with some important improvements and generalizations, as we explain shortly. In particular, the term tether-method is not appropriate for non-spherical particles. Instead, we prefer to continue to think of this as a cell-method, but with a wiser choice of cell than a Voronoi polyhedron. We will call the method the Bounding Cell MD (BCMD) algorithm. It fits directly into the collision-driven MD algorithm that we developed in detail in Ref. [9].

3.1. Basic algorithm

The algorithm for performing hard-particle MD described in Ref. [9] is collision-driven (event-driven), meaning that the algorithm makes predictions on when two particles collide and then jumps from collision to collision asynchronously. For the purposes of improving the computational efficiency of the algorithm, near-neighbor lists (NNLs) were introduced in Ref. [9] through the concept of a *bounding neighborhood*, which we will call *bounding cells* in this context. Namely, for a given snapshot configuration of the packing, each particle is surrounded by a cell that has exactly the same shape as the particle itself, but is scaled uniformly by a scaling factor $\mu = 1 + \Delta\mu$. The volume of the cell is thus $V_c = \mu^d V_p$, where V_p is the volume of the particle. Two particles that remain within their bounding cells may only collide if the bounding cells overlap. Therefore, each particle only needs to predict collisions with the particles whose bounding neighborhoods/cells overlap with its own (kept in a near-neighbor list), and also predicts collisions with its own bounding cell. The BCMD algorithm uses exactly this same machinery with one important difference: When a particle collides with its cell, instead of rebuilding its list of near neighbors (as done in Ref. [9]), the particle bounces off the cell wall as if the cell had hard walls.

This is just like the single-occupancy cell (SOC) system used in Ref. [2], however, with cells that do not necessarily cover space and which have the same shape as the particles, rather than being complex polyhedra. We now focus on solid-like systems, meaning that there is no or very little free diffusion, so that over long periods of time the particles do not move far away from their initial positions (i.e., the centers of the cells). When the cells are very large, that is, $\mu = \mu_{max} \gg 1$, the SOC system is indistinguishable in its thermodynamic properties from the unconstrained system. In the limit $\mu \to 1$, the cells will become disjoint and the system becomes a collection of N independent particles, which can be treated analytically. We will assume that there exists a $\mu_{min} > 1$ for which the cells are fully disjoint. This can always be assured by preparing the initial state more carefully or by shrinking the particles slightly.

The basic idea of the BCMD algorithm is to connect the two states, one with large-enough and the other with small-enough cells, via a thermodynamically reversible (quasi-equilibrium) path. We do this in the our MD simulation by simply slowly reducing the scaling factor during the course of the MD simulation

$$\mu = \mu_{max} - \gamma_\mu t$$

with a constant *cell reduction rate* γ_μ. The algorithm developed in Ref. [2] already has allowance for a potentially changing shape of colliding particles, and therefore the introduction of a bounding cell with a changing shape poses no additional technical issues. During the course of the MD, we can measure the average reduced pressure on the walls of a cell $p_c = P_c V_c / kT$ and then obtain the change in free energy as the work done in shrinking the cells

$$f_c(\Delta\mu_{min}) - f = \int_{V_c^{max}}^{V_c^{max}} p_c \frac{dV_c}{V_c}. \tag{6}$$

We will assume that one can calculate $f_c(\Delta\mu)$ theoretically, and thus Eq. (6) gives us f. For example, for spheres of unit diameter, we have the trivial result

$$f_c(\Delta\mu) = -d_f \ln \Delta\mu - \ln V_p, \tag{7}$$

and, in general, for particles with unit dimensions,

$$f_c(\Delta\mu) = -d_f \ln \Delta\mu - f_c^J, \tag{8}$$

where f_c^J is a constant which depends on the exact particle shape, $f_c^J = \ln(\pi/6)$ for spheres.

The BCMD method is inspired by and closely related to the tethered-spheres method of Speedy [12]. Speedy describes this method for spheres as having the center of each particle tied with a tether to its initial position, and then considers changing the length of the tether in fixed finite increments, performing MD, and measuring the average tether force. He also points out the implicit presence of cells. One naturally extends the algorithm to non-spherical particles by adopting the cell picture. Additionally, we continuously change the cell size with time and adjust our MD algorithm accordingly, rather than using fixed finite steps. This offers more than just computational convenience. Namely, it gives a control parameter, γ_μ, which can be used to control the accuracy of the results: reducing γ_μ improves the accuracy by both allowing for better equilibration and by increasing the number of collisions processed (and thus the overall statistical accuracy). More importantly, as we will explain in the next section, one can directly obtain the change in free energy from the change in kinetic energy of the system, thus obviating the need to define and measure[3] "pressure" and integrate it numerically after the simulation has finished, using potentially erroneous interpolation. This not only improves the accuracy, but also enables one to calculate change in "free energy" in non-equilibrium processes where dynamics does matter and one cannot stop the simulation at specific points, such as the production of glasses by (relatively rapid) quenching.

We note in passing that recent Monte Carlo switch methods can more directly (and thus accurately) measure the difference in free energies between two states by directly switching from one state to the other [24]. It would be interesting to investigate such methods where the two states are the large and small cell states.

3.2. Elastic collision law

An important detail which has not been discussed carefully enough in the literature is the collision law for particle–particle and particle–wall collisions in the presence of a deforming particle shape or deforming wall. The collision law that we use is an elastic one, in the following sense: linear and angular momentum are conserved, and the direction of the *relative* normal surface-to-surface velocity $v_\perp$ at the point of contact is reversed upon collision (but the magnitude is unchanged). It is most convenient to consider binary collisions only and then just take the limit that the "mass" of a hard wall goes to infinity. This collision law corresponds to a non-dissipative collision during which a purely normal exchange of momentum $\Delta\pi_c$ occurs and an additional work $W_c = v_\perp \Delta\pi_c$ is performed in order to maintain the rate of deformation of the particle/wall shape during the collision. Therefore, even though at first sight such collisions are not conserving kinetic energy, they are in fact conserving if one takes into account the work done by external "agents" to change the shape of the particles, cells, or container. The first study that we are aware of where such collisions are considered is Ref. [25], and there an adjustable parameter h is left in the collision law, and its choice is considered free. In fact, the actual choice made there corresponds to the above "conserving" (elastic) collision law, and is thus the best choice possible.

Using energy-conserving collisions enables us to calculate the change in free energy during a continuous transformation of the system by simply considering the change in kinetic energy of the particles. Examples are the change in kinetic energy as the cells are shrunk during the cell method, or as particles are grown in size in order to produce jammed/glassy packings, or as the particles go from non-spherical to spherical, or as the shape of the simulation box shears from cubic to sheared-cubic, etc. Virtually any quasi-equilibrium transformation can be studied by simply performing it using collision-driven MD and letting the kinetic energy K increase or decrease spontaneously, to give the change in free energy

$$\Delta f = \frac{d_f}{2} \ln \frac{K}{K_0}. \tag{9}$$

In Appendix A, we derive this formula for the BCMD method by looking at the algorithm in high-dimensional configuration space, giving us a unique perspective on the key elements of the algorithm that enable measurement of configurational volume to be done by performing (molecular) dynamics.

[3] For example, for non-spherical particles the force exerted by the particle on the walls of the cell is non-uniform, so that in principle a pressure tensor needs to be considered.

3.3. Algorithmic details

We now turn to some technical details needed when using the BCMD algorithm in practice. The first concerns the choice of boundary conditions. We have employed periodic boundary conditions here, which gives d trivial translational degrees of freedom to the unconstrained system. However, when cells are present, they are fixed in space, breaking the translational symmetry. The usual approach to eliminating trivial translations is to freeze the center of mass of the particle system. In traditional conservative MD simulations, this is done easily by simply ensuring that the initial velocities add to zero. However, collisions with the hard walls of the bounding cells do not conserve linear momentum. This leads to an artificial increase of the collision rate of the particles with the cells, particularly at high densities (i.e., near jamming), because the center of mass oscillates as the excess linear momentum is distributed among the particles through binary collisions. Speedy proposed to artificially enforce a frozen center of mass by correcting the velocity of all of the particles whenever a particle collides with a bounding cell. This is rather inefficient; instead, we have chosen to evaluate the kinetic energy K in the center-of-mass system. For sufficiently large systems, the corrections due to center-of-mass oscillations are small. Another way to eliminate trivial translations is to freeze one particle (give it infinite mass), which is especially useful near jamming. The two methods are not equivalent in terms of free energy. The difference in free energy due to this change of boundary conditions is shown to be $\mathrm{d}\ln N/N$ in Appendix B.

The second technical issue concerns that of adjusting the reduction rate γ_μ. The rule of thumb is to keep it small enough so that the actual linear velocity of the moving cell walls is small (say 10^{-3} times smaller) compared to the average particle velocity. Keeping γ_μ constant, however, uses too much computer time for large μ, a region which actually contributes little to the total configurational volume, and too little on small μ, where more precision is actually required. We have chosen to implement a periodic adaptive change of the reduction rate[4]

$$\gamma_\mu(\mu) = \gamma_\mu(\mu_{\max})\left(\frac{\Delta\mu}{\Delta\mu_{\max}}\right)^{\vartheta},$$

where ϑ is an exponent, which we have usually kept in the range 0.25–1, depending on the size of the system and the initial $\gamma_\mu(\mu_{\max})$ as well as the ratio $\Delta\mu_{\min}/\Delta\mu_{\max}$. It is important to consider the convergence of the BCMD method in more detail using existing powerful mathematical techniques and try to determine a theoretically sound $\gamma_\mu(\mu)$ that would provide a *desired* total error in f with reasonable confidence.[5] At present, we do not have such a theory and therefore are unable to quote rigorous error bars on our results other than statistical fluctuations among samples and also estimated errors from different runs with successively smaller $\gamma_\mu(\mu_{\max})$ or larger ϑ.

The final technical point concerns the actual practical implementation of the BCMD algorithm for ellipses/ellipsoids. As explained in the second part of Ref. [9], the numerical calculation of overlap potentials in the case of one ellipsoid contained inside another is numerically unstable and causes difficulties in the correct prediction and processing of collisions with the bounding cells. While the occasional numerical failures can be tolerated when the bounding neighborhoods are used only for speeding up the neighbor search in the MD algorithm, they become an insurmountable obstacle with the cell method, especially when the cells are disjoint or nearly disjoint. This is because a wrong collision prediction can lead to a particle leaving its cell permanently. We have not really found a satisfactory solution to this problem, and have been forced to use reduction rates γ_μ sufficiently fast so that such failures are unlikely to appear. However, the reduction rate must still be small enough to ensure that the linear velocity of the moving cell walls is small compared to the average particle velocity.

An additional technical difficulty when dealing with ellipsoids is the fact that there is no analytical equivalent to Eq. (7). One possibility is to calculate f_c for a particle inside its cell numerically by following a reversible path to a known system. Two possibilities include the case of an infinitesimally small particle, reducing to

[4] Note that in the actual implementation γ_μ is updated periodically, rather than continually.

[5] It is reasonable to assume that an error of the order $\ln N/N$ is acceptable, since finite-size effects are of this order [26]. This means that the configurational volume only needs to be determined to within a factor of $\ln N$.

a one-particle ideal gas inside a container of volume V_c, or the case of a spherical particle inside a spherical cell. The first system can be reached by shrinking the size of the particle slowly, and the second by reducing the asphericity. We have implemented both options in our MD codes, however, as explained above, numerical difficulties are a problem. For this reason we (semi)analytically consider the case of an ellipse of aspect ratio $\alpha = 2$ inside a bounding cell in Appendix C, to obtain $f_c^J \approx 2.269$. We have verified this result (to within the precision possible) with the MD algorithm by calculating the change in free energy as the ellipses and the cells were slowly transformed into disks while keeping $\Delta\mu$ fixed by shrinking the larger semiaxis to unity. Namely, for small-enough $\Delta\mu$, the change in free energy during such a transformation is known analytically to be

$$\Delta f_{\text{sphere}} = -\ln[\pi(\pi\Delta\mu^2)] - [-3\ln\Delta\mu - f_c^J] = \ln\Delta\mu + f_c^J - 2\ln\pi,$$

where we have used the fact that a disk has full rotational freedom (contributing a factor of π to the configurational volume).

4. Results

In this section, we give an illustration of the BCMD algorithm as applied to a hard-sphere liquid near the freezing point. We then present the first testing of the BCMD algorithm against rigorously-known free energies by applying it to isostatic jammed systems. For these systems, as explained in Section 2, the free-energy in the jamming limit can be found from the volume of a simplex polytope, which can be calculated exactly easily even for large systems. In the jamming limit, we choose to freeze one particle in order to eliminate trivial translations, so that the effective number of particles N is one less than the true number of particles. Assuming that we start the cell method at exactly the jammed configuration $\mathbf{R}_J$, the cells will become disjoint when $\Delta\mu_{\min} = \delta$. The total change in free energy during the course of shrinking the cells is

$$\Delta f = \frac{d_f}{2}\ln\frac{K}{K_0} = (-f_c^J - d_f\ln\delta) - (-d_f\ln\delta - f_J) = f_J - f_c^J, \tag{10}$$

where we recall that $f_J = (N-1)^{-1}[\ln|\mathscr{P}_{\mathbf{x}}|]$, which can be calculated easily if $\mathscr{P}_{\mathbf{x}}$ is a simplex, and f_c^J is known for a given particle shape. We use Eq. (10) to rigorously validate and test the accuracy of the BCMD algorithm. As an initial test, we compare against the highest-precision MC results for hard-sphere crystals that have appeared in the literature. In other work, we apply the validated BCMD algorithm to dense liquid and glassy systems further from the jamming point in order to better understand the thermodynamics of hard-particle metastable liquids and glasses [10,11].

4.1. Dense hard-sphere liquid

As an illustration of the BCMD algorithm we apply it to a system which is at the limit of the method's applicability: a dense hard-sphere liquid near the freezing point, at $\phi = 0.5$. This is still a liquid and thus the particles diffuse freely given sufficient time, and the cell method is not rigorously applicable. However, adding the cells stabilizes the liquid in the neighbourhood of its initial configuration for long periods of time, thus allowing the measurement of the free-energy for a metastable cell-constrained liquid (CCL). This free-energy is certainly larger than that of the unconstrained liquid, which has more free volume available to explore. If one assumes that one can divide this liquid free volume into more-or-less N_b equivalent "basins", each basin corresponding to a single "glassy" jammed configuration, then the loss of entropy due to the presence of the cells would be of the order of $N^{-1}\ln N_b$. This assumption about dividing configuration space into statistically equivalent compartments or basins, though commonly used in the literature, has not really been justified for the hard-sphere system (where entropy cannot be "turned off" by going to zero temperature).

In Fig. 1, we show the results of the cell method as applied to a stable liquid. We show both the pressure on the cell walls p_c, which dominates at $\mu = \mu_{\min}$, and the pressure p, which dominates at $\mu = \mu_{\max}$, when it approaches the true (unconstrained) liquid pressure. It is seen that the cell-wall pressure shows a minimum, as first observed in Ref. [12], when $\mu \approx 2$, i.e., when a bounding cell corresponds to the exclusion sphere of its particle in the initial liquid configuration. For $\mu > 2$ it appears that particle rearrangements take place which increase p_c. Even though p_c has a minimum, it remains positive throughout due to the diffusion of

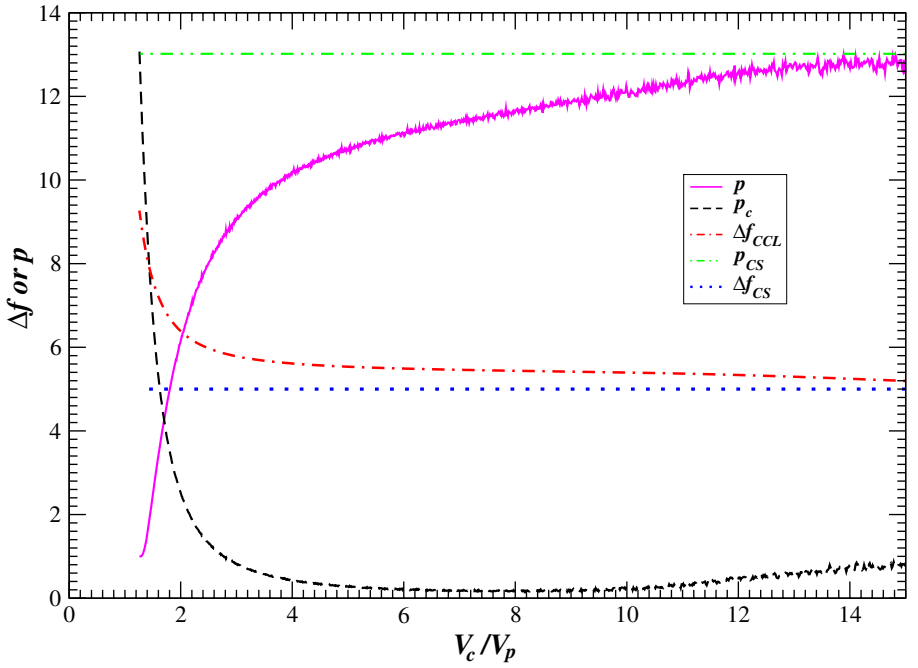

Fig. 1. Illustration of the BCMD algorithm for a dense equilibrium hard-sphere liquid close to the freezing point, $\phi = 0.5$. We show as a function of the relative size of bounding cells, the pressure p as well as the cell-wall pressure p_c, along with the calculated excess free energy of the cell-constrained liquid $\Delta f_{CCL}(\mu)$. The results from the semiempirical CS EOS is shown for comparison. It is seen that the pressure on the cell walls goes through a minimum but is always positive due to the free diffusion of the particles. The values of p_c for large μ are more difficult to measure accurately, since they depend on particle diffusion and they have not been studied carefully.

the particles, and therefore one cannot measure the true free-energy of the liquid using the BCMD algorithm. Instead, we show in Fig. 1 the excess free-energy of the cell-constrained liquid relative to the ideal gas,

$$\Delta f_{\mathrm{CCL}}(\mu) = f(\mu) - f_{\mathrm{ideal}} = \Delta f_{\mathrm{c}}(\Delta\mu_{\mathrm{min}}) - \mathrm{d}\int_{\mu_{\mathrm{min}}}^{\mu} p_{\mathrm{c}}\frac{\mathrm{d}\mu}{\mu}.$$

Here the ideal-gas free energy is trivially

$$f_{\mathrm{ideal}} = -\frac{1}{N}\ln\frac{V^N}{N!} \approx -\ln\frac{V}{N} - 1 = -\ln\frac{V_{\mathrm{p}}}{\phi} - 1 \tag{11}$$

and therefore

$$\Delta f_{\mathrm{c}}(\Delta\mu) = -\ln\Delta\mu^d V_{\mathrm{p}} + \ln\frac{V_{\mathrm{p}}}{\phi} + 1 = -\ln(\phi\Delta\mu^d) + 1. \tag{12}$$

In the figure, we compare $\Delta f_{\mathrm{CCL}}(\mu)$ to the results predicted by the relatively-accurate Carnahan–Starling (CS) equation of state (EOS) for the liquid [27],

$$p_{\mathrm{CS}} = \frac{1+\phi+\phi^2-\phi^3}{(1-\phi)^3} \quad \text{and} \quad f_{\mathrm{CS}} = \int_o^{\phi}\frac{p-1}{\phi} = \frac{\phi(4-3\phi)}{(1-\phi)^2}.$$

We note in passing that closer to the jamming limit a more careful analysis of the contribution to the free energy by rattling particles is needed, and give details in Appendix D.

While $\Delta f_{\mathrm{CCL}}(\mu \approx 2)$ is a reasonable approximation to the true liquid free energy at such high liquid densities, the difference between the two, called *communal entropy* by Kirkwood for his single-occupancy cell liquid model, is not zero and was estimated a long time ago [28]. Additionally, due to somewhat arbitrary choice of the cell size (unlike in Kirkwood's model where the cell partitioning is fixed), the exact value is not well-

defined, and therefore interpretations in terms of number of "inherent-structures" that the liquid samples are questionable. We will discuss these issues in significant detail in subsequent work [11].

4.2. Hard-sphere crystals

The entropy of hard-sphere crystals as a function of density has approximately been known from the early days of computer simulations [28]. Interest in the problem has re-surfaced recently and there have been several attempts to determine whether the FCC or the HCP crystal has lower free energy (and is thus the stable solid phase) [2–4,23,29,30]. The difference between the two is very small and the literature is filled with contradictory claims and underestimated error bars. The most accurate results are those produced by MC switch algorithms, which do not determine an absolute free-energy but rather directly measure the entropy difference between FCC/HCP, producing a difference of about 1.1×10^{-3} N kT in favor of FCC configurations in the jamming limit [3].

The results for the pressures and absolute value of the free energies have been summarized and processed in Ref. [29], and the most precise quoted MC result for the excess free energy of the FCC crystal over the ideal gas is close to the melting point, $\Delta f_{\mathrm{FCC}}(\phi = 0.545) = 5.91916(1)$. At the same density, the BCMD algorithm with $\Delta\mu_{\max} = 1$, $\gamma_\mu(\mu_{\max}) = 0.001$ and $\vartheta = 1$ produces 5.919(0), which is in excellent agreement. In the jamming limit, from the data in Ref. [29] we estimate

$$[f_{\mathrm{J}} - f_{\mathrm{c}}^{\mathrm{J}}]_{\mathrm{FCC}} = 2.160 \pm 0.001,$$

where the exact error bars are difficult to cite since most of the focus has been near the melting point rather than close packing. Our most precise BCMD runs have involved about 10,000 spheres at $\delta = 10^{-6}$ and $\Delta\mu_{\max} = 10^{-5}$ with $\gamma_\mu(\mu_{\max}) = 0.001$ and $\vartheta = 0.5$, giving $[f_{\mathrm{J}} - f_{\mathrm{c}}^{\mathrm{J}}]_{\mathrm{FCC}} = 2.1599 \pm 0.0005$ and $[f_{\mathrm{J}} - f_{\mathrm{c}}^{\mathrm{J}}]_{\mathrm{HCP}} = 2.1593 \pm 0.0005$, where as pointed out previously the true error bars are not known. The excellent agreement between our results and the published ones serves as a validation of the algorithm and our implementation. Unfortunately, the true volumes of the jamming polytopes corresponding to the jamming limit cannot be calculated exactly for anything but small systems [4], since their combinatorial complexity is exponential.

The difference in free energy between the FCC and HCP lattices as calculated with the BCMD algorithm is of the same sign and order of magnitude as results in the literature. However, the error bars are significant and although it is possible to run longer and larger simulations to improve them we believe that without a rigorous error analysis one should not really engage in trying to decide the "winner" among these two lattices. Additionally, the impact of vacancies needs to be accessed more carefully. Furthermore, the HCP lattice does not have full cubic symmetry and therefore the crystal of minimum free energy is slightly compressed along the hexagonal symmetry axis [30]. Preliminary calculations indicate that both of these effects produce corrections that are about an order of magnitude smaller than the reported difference between FCC and HCP, however, more rigorous results are lacking. Finally, the importance of randomly stacked arrangements is not obvious, despite the natural assumption that one of the two extremal stacking arrangements (ABA and ABC) will produce the minimal free energy.

It is interesting to observe that the BCMD method works remarkably well for a solid like the FCC crystal, even at densities as low as the melting density. This is because the displacements of the particles from the ideal lattice positions are small (usually Gaussian in density functional approximations) and thus well-localized around the equilibrium locations. This makes $p_{\mathrm{c}}(\Delta\mu)$ a rapidly (faster than exponential) decaying function which is easy to integrate accurately with little computational effort, as illustrated in Fig. 2. This is not the case for disordered packings of monodisperse spheres, where the particle displacements are significant and $p_{\mathrm{c}}(\Delta\mu)$ decays slowly in a power-law manner. Two-dimensional crystals that lack long-range translational order are also expected to show significant particle delocalization at densities away from the jamming density.

4.3. Isostatic jammed packings: spheres

We have generated isostatic disordered jammed sphere packings of $N = 1000$ spheres using the procedures described in Ref. [13]. These packings have a number of *rattlers*, particles which are free to move inside a cage

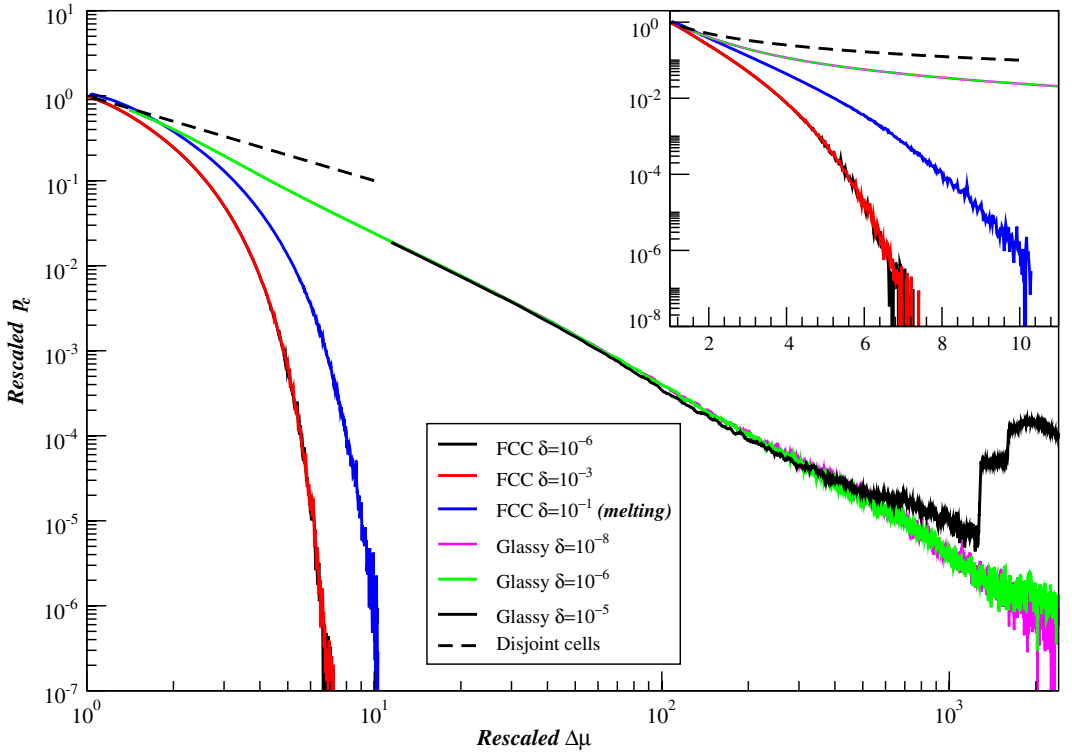

Fig. 2. Rescaled values of the cell-wall pressure $\widetilde{p_c} = \delta p_c$ as a function of rescaled $\Delta\tilde{\mu} = \Delta\mu/\delta$ for several different values of δ for both an FCC crystal packing ($N \approx 10^4$) and an isostatic disordered packing ($N \approx 10^3$, see Section 4.3). We also show for comparison the expected asymptotic dependence in the limit of disjoint cells, $\widetilde{p_c} = \Delta\tilde{\mu}^{-1}$, as well as a semi-logarithmic scale view of the data in the inset. In the jamming limit, where the polytope picture applies, we expect these rescaled curves to follow a universal curve independent of δ.

of jammed particles. We remove these rattlers[6] and freeze one particle before applying the BCMD method in order to make the packings fit the simplex picture exactly, and then we compute the exact free-volume in the jamming limit from the volume of the simplex using Eq. (3). As an illustration, we consider one of these packings of $N = 978$ particles (1000 particles with the rattlers), and get $f_J - f_c^J \approx 4.9479$ (in the frozen center-of-mass coordinate system $f_J - f_c^J \approx 4.9690$). Table 1 shows the results obtained from the BCMD algorithm at $\delta = 10^{-8}$ with several different choices of the main parameters, illustrating the excellent agreement with the exact result, especially in the limit of infinitely long runs.[7] The primary error is likely due to statistical fluctuations in the kinetic energy due to the relatively small number of particles. It is important to note that the simplex polytopes for disordered packings are very elongated in certain directions and therefore require significantly larger $\Delta\mu_{max}/\delta$ than crystal packings.

In Fig. 2, we show the cell-wall pressure as a function of the cell size, illustrating the fact that it decays very slowly. In fact, this particular isostatic packing (recall, after rattlers have been removed) unjams when $\delta \approx 10^{-5}$ without the presence of the cell walls to stabilize it. The difference between the crystal and glassy packings is striking. For the crystal packings, $\widetilde{p_c}$ decays at least exponentially, even at densities as low as the melting point ($\phi \approx 0.545$), making it easy to obtain the free energies. However, for the disordered packings the decay is power-law like, with long tails which are more difficult to integrate accurately. Studies of glasses fur-

[6] The rattler contribution to the change in free energy during the densification of packings is discussed in Appendix D. Here we remove the rattlers in order to obtain truly isostatic packings. However, rattlers cannot always be removed from consideration, for example, they contribute essentially to the recently-observed vanishing of long-range density fluctuations in disordered jammed hard-sphere packings.

[7] One could potentially improve the precision by extrapolating to, for example, $\gamma_\mu(\mu_{max}) \to 0$, however here we are primarily interested in testing the method rather than obtaining the most accurate result.

Table 1
Results of the BCMD algorithm for an isostatic disordered jammed sphere packings of $N = 1000$ spheres, with different parameters for the algorithm

δ	$\Delta\mu_{\max}$	$\gamma_\mu(\mu_{\max})$	ϑ	$f_J - f_c^J$
10^{-8}	2.5×10^{-5}	0.1	1.00	4.9476
10^{-8}	2.5×10^{-5}	0.01	0.25	4.9480
10^{-8}	1.5×10^{-5}	0.001	0.25	4.9458
10^{-8}	2.5×10^{-5}	0.01	0.50	4.9493
10^{-8}	2.5×10^{-5}	0.01	0.75	4.9485
10^{-8} (frozen CM)	2.5×10^{-5}	0.01	0.50	4.9624
10^{-7}	2.5×10^{-4}	0.01	0.25	4.9498
10^{-6}	2.5×10^{-3}	0.01	0.25	4.9414

The rattlers were removed and one particle was frozen, except in one case where the center of mass was frozen. In principle the exact answer $f_J - f_c^J = 4.9479$, as calculated from the volume of the jamming simplex, should be reached for infinitely long runs as $\delta \to 0$. Typical running times are of the order of several hours to a day on an 1666 MHz AMD Athlon PC running Linux.

ther away from the jamming point will be presented in separate work [11]; here we will focus on the region where the simplex picture applies.

4.4. Isostatic jammed packings: ellipses

As we discussed already, non-spherical particles pose problems to the polytope picture in general and cannot usually be analyzed within this picture even in the jamming limit. However, it is possible to artificially make isostatic jammed packings that do fit into the polytope picture (i.e., first-order rigid packings [22]). The idea here is to obtain a packing which has $6 - 2/N \approx 6$ contacts per particle, since this is the number required for an isostatic packing ($M = N_f = 3N - 2 + 1 = 3N - 1$). We cannot use a crystal packing here since

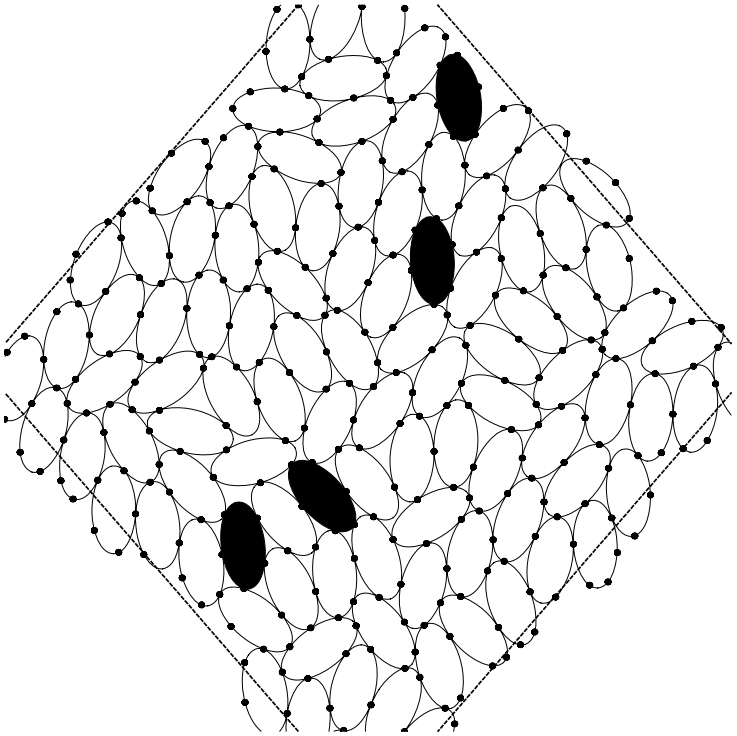

Fig. 3. A sample isostatic jammed (first-order rigid) packing of $N = 96$ free and four frozen ellipses of aspect ratio $\alpha = 2$, used to test the BCMD algorithm on non-spherical particles. This packing was produced using a complicated artificial procedure as described in the body of the paper, and is not typical of disordered ellipse packings, which have fewer contacts per particle.

those have exactly six contacts per particle and are thus hyperstatic by one contact, and typical disordered packings of ellipses are usually rather hypostatic, having too few contacts for first-order rigidity. We therefore started with a triangular lattice of $N = 100$ disks, replaced each disk with an ellipse of aspect ratio 2, and then compressed the packing using MD to jamming to obtain a partially disordered packing. Even these packings had $M < 3N - 1$. However, by freezing 4 of the particles we were able to obtain packings which had matched number of degrees of freedom and contacts. We then calculated the volume of the simplex, obtaining $f_J - f_c^J = 3.6693$ for the packing illustrated in Fig. 3. Running the BCMD algorithm at $\delta = 10^{-4}$ with

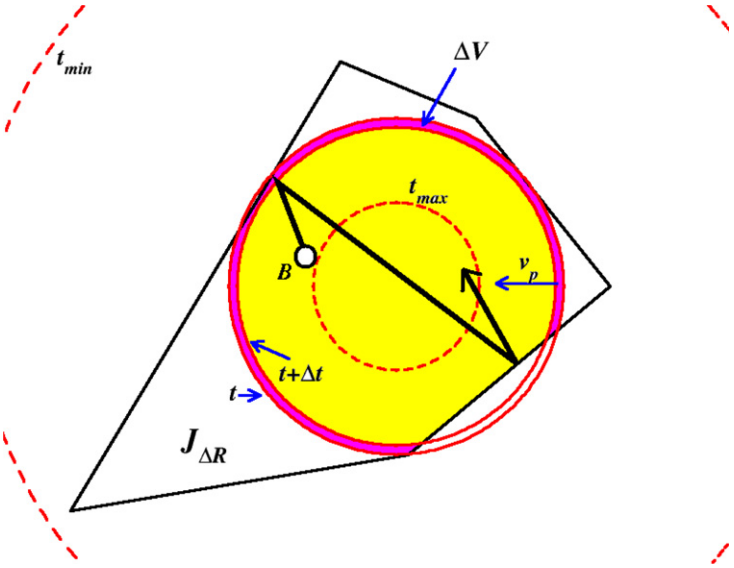

Fig. 4. An illustration of the BCMD algorithm in a ficticious two-dimensional configuration space. The surface area of the polygon ($\mathscr{J}_{\Delta\mathbf{R}}$) is obtained by intersecting it with a shrinking disk of radius $\xi(t)$ centered inside the polygon [$\widetilde{\mathscr{J}}_{\Delta\mathbf{R}}$], and integrating the surface area (colored purple) of the intersection region ($\widehat{\mathscr{J}}$, shaded in yellow). This surface area is measured from the pressure exerted on it by a ball $\mathscr{B}$ bouncing elastically inside the intersection region. (For interpretation of the references in colour in this figure legend, the reader is referred to the web version of this article.)

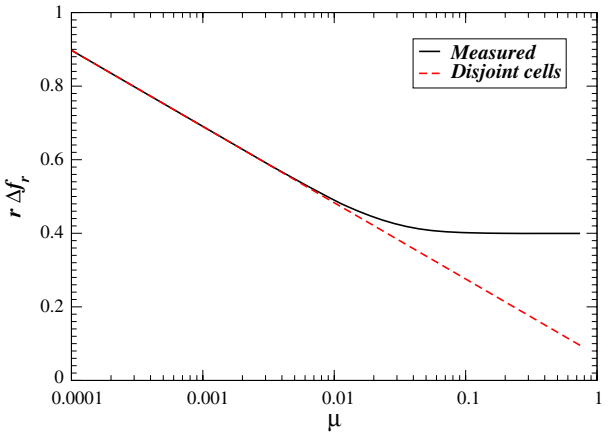

Fig. 5. The measured contribution of the 30 rattlers to the excess free energy for a jammed disordered packing of $N = 1000$ spheres, $r\Delta f_r(\mu)$, as a function of the bounding cell relative size. The non-rattling particles, i.e., the particles in the jammed backbone, were frozen. For small μ the rattler cells are disjoint from the backbone in which case the free energy is known analytically (red line). For large μ the presence of the cells does not make a difference and one can extract the appropriate $r\Delta f_r(\mu) \approx 0.4$ to use in Eq. (D1). (For interpretation of the references in colour in this figure legend, the reader is referred to the web version of this article.)

$\Delta\mu_{\max} = 1.5 \times 10^{-2}$ with $\gamma_\mu(\mu_{\max}) = 0.001$ and $\vartheta = 0.5$ gave $f_J - f_c^J = 3.61 \pm 0.01$, in reasonable agreement with the known answer. Higher accuracy is hard to achieve at present due to numerical difficulties in the implementation discussed previously. We note that when using a frozen particle to eliminate trivial translations only, its centroid must be fixed, but not its orientation, since the orientation of the coordinate system is fixed by the orientation of the periodic unit cell.

An additional possibility that deserves further investigations is using transformations of the particle shape without any cell models in order to measure free energies. Examples would include superellipses transforming into ellipses, or ellipses transforming into spheres, etc., while measuring the change in kinetic energy. The difficulty in such simulations is the identification of reversible paths free of discontinuous phase transitions. However, the possible increased computational efficiency as well as the ability to study a whole range of particle shapes in one simulation make the method very attractive.

5. Conclusions

We developed an MD algorithm for measuring the free energy of systems of hard particles where diffusion is negligible. By exploiting free-volume theories for the jamming limit of hard-particle packings we were able to exactly calculate the asymptotic behavior of the free energy of model disordered jammed systems, namely isostatic jammed sphere and ellipsoid packings. This provided us with a rigorous verification of the numerical accuracy of the BCMD algorithm. Several technical points were developed in the Appendices, paving the way to answering several open questions. In particular, a quantative understanding of the statistical and systematic errors in the BCMD algorithm is missing. Additionally, a quantitative understanding of the connection between hard-particle systems (where free energy is the volume of a bounded high-dimensional body) and low-temperature soft-particle systems (where free energy is a weighted volume integral) is important to elucidating the utility and limitations of hard-particle models of real materials. Elsewhere [10,11], we have successfully applied the algorithm presented here to demonstrate that there is no ideal-glass transition for binary hard disks.

Acknowledgement

This work was supported by the National Science Foundation under Grant No. DMS-0312067.

Appendix A. Billiards algorithm for volume calculation

In this Appendix, we examine the BCMD algorithm in high-dimensional configuration space in order to understand how it actually measures the free volume and also how it can be applied as a general algorithm for measuring the volume of a (nearly) convex body in high dimensions. We also compare it to known efficient algorithms for measuring the volume of a convex body in high dimensions.

The motion of a nearly jammed hard-particle system in N_f-dimensional configuration space corresponds to a (point) billiard ball $\mathscr{B} \in \mathscr{R}^{N_f}$ elastically bouncing inside the nearly convex closed body $\mathscr{J}_{\Delta\mathbf{R}}$ whose volume $\mathscr{V} = |\mathscr{J}_{\Delta\mathbf{R}}|$ we wish to calculate. We assume here that the dynamics of the ball is ergodic and can be analyzed within classical equilibrium thermodynamics. The ball exerts a *uniform* pressure $P = k_B T/\mathscr{V}$ on the walls when averaged over sufficiently many collisions with the walls, where the temperature $k_B T = 2K/N_f$ measures the kinetic energy of $\mathscr{B}$. The assumption of ergodicity is non-trivial and is usually assumed to hold when all of the walls of $\mathscr{J}_{\Delta\mathbf{R}}$ are semidispersing (concave) [31], which is true only for sphere packings. Physically, ergodicity is often attributed to the presence of a large number of particles. However, even with a large number of non-spherical particles the dynamics of $\mathscr{B}$ can be highly non-trivial and non-uniform.

The elastic nature of the ball implies that both the kinetic energy and the component of the momentum parallel to the wall are conserved upon collisions with a stationary wall of $\mathscr{J}_{\Delta\mathbf{R}}$. If a wall is moving due to, for example, growth in the size of the particles, when $\mathscr{B}$ collides with the wall, it gets a velocity boost in the direction normal to the wall such that the normal velocity of the ball relative to the wall is reversed,

$$v_\perp^{\text{after}} - v_\perp = -(v_\perp^{\text{before}} - v_\perp),$$

where $v_\perp$ denotes the (local) normal velocity of the wall. This kind of dynamics ensures that the ball never sticks to the wall and also implies energy conservation in the following sense: the change in kinetic energy of the ball is

$$\Delta K_c = \frac{m}{2}(v_\perp^{\text{after}} - v_\perp^{\text{before}})(v_\perp^{\text{after}} + v_\perp^{\text{before}}) = v_\perp \Delta\pi_c,$$

where $\Delta\pi_c$ is the momentum exchanged between the ball and the wall. Therefore, ΔK_c is exactly the work done by the moving wall against the force exerted on it by the bouncing ball.

Now consider adding constraints on the displacements of the particles in addition to the non-overlap conditions with some parameter ξ that determines how strong are these additional constraints. In isolation, the additional constraints limit the configuration to some neighborhood $\widetilde{\mathscr{J}}_{\Delta\mathbf{R}}(\xi)$ around $\mathbf{R}_J$, so that $\widetilde{\mathscr{J}}_{\Delta\mathbf{R}}(\xi \to 0) = \{\mathbf{R}_J\}$ and $\widetilde{\mathscr{J}}_{\Delta\mathbf{R}}(\xi \to \infty) = \mathscr{R}^n$. For example, in our MD algorithm, we add the constraints that each particle remain within its bounding cell, and can identify $\xi = \Delta\mu$. In a more general situation, we could simply add the constraint that the configuration remain within a hypersphere of radius ξ centered at $\mathbf{R}_J$. Here we will assume that the volume $|\widetilde{\mathscr{J}}_{\Delta\mathbf{R}}(\xi)|$ is known. The resulting available region of configuration space $\widehat{\mathscr{J}} = \widetilde{\mathscr{J}}_{\Delta\mathbf{R}} \cap \mathscr{J}_{\Delta\mathbf{R}}$ interpolates between $\mathscr{J}_{\Delta\mathbf{R}}$ for sufficiently large $\xi = \xi_{\max}$ and $\widetilde{\mathscr{J}}_{\Delta\mathbf{R}}$ for sufficiently small $\xi = \xi_{\min}$. A two-dimensional illustration is provided in Fig. 4.

Our algorithm for measuring $|\mathscr{J}_{\Delta\mathbf{R}}|$ essentially consists of dynamically decreasing $\xi(t)$ from $\xi_{\max}$ to $\xi_{\min}$ while following the collision dynamics of the billiard ball, and simply measuring the relative change in kinetic energy K/K_0 during the process. This change in kinetic energy arises because of the motion of the walls of $\widetilde{\mathscr{J}}_{\Delta\mathbf{R}}$ as ξ changes. Namely, consider the short time interval from t to $t + \Delta t$ during which the volume $\mathscr{V}(\xi) = |\widehat{\mathscr{J}}(\xi)|$ decreases by $\Delta\mathscr{V} = Sv_\perp\Delta t$, where S is the surface area of $\widetilde{\mathscr{J}}_{\Delta\mathbf{R}}$ contained within $\mathscr{J}_{\Delta\mathbf{R}}$. The increase in kinetic energy of $\mathscr{B}$ during this interval is

$$\Delta K = v_\perp \Delta\pi = \frac{\Delta\pi}{S\Delta t}\Delta\mathscr{V} = P\Delta\mathscr{V} = k_B T\frac{\Delta\mathscr{V}}{\mathscr{V}(\xi)} = \frac{2K}{N_f}\frac{\Delta\mathscr{V}}{\mathscr{V}(\xi)}.$$

Taking the limit $\Delta t \to 0$, we get a differential equation whose solution gives the volume $\mathscr{V} = \mathscr{V}(\xi_{\max})$,

$$\ln\frac{\mathscr{V}}{\mathscr{V}_{\min}} = \frac{N_f}{2}\ln\frac{K}{K_0}, \tag{A1}$$

where $\mathscr{V}_{\min} = \mathscr{V}(\xi_{\min}) = |\widetilde{\mathscr{J}}_{\Delta\mathbf{R}}(\xi_{\min})|$ is known. Eq. (A1) was used to obtain Eq. (9).

The basic elements of the algorithm are essentially identical to well-known polynomial algorithms for computing the volume of a convex body in high dimensions [18]. The majority of these algorithms (other than the best known algorithm from Ref. [32]) use a random walk through the convex body $\widehat{\mathscr{J}}$ to essentially estimate the fraction of the surface area of $\widetilde{\mathscr{J}}_{\Delta\mathbf{R}}$ that is contained in $\widehat{\mathscr{J}}$. The total volume is then calculated as a product of such fractions, i.e., the logarithm of the volume is calculated as a sum (i.e., an approximation to the integral of the surface area). In our algorithm, we use (ergodic) molecular dynamics to estimate and integrate the fractions as ξ is changed dynamically. We believe that the powerful mathematical techniques developed for the analysis of random walk algorithms together with techniques from theory of ergodic billiards could be applied to analyze the BCMD algorithm and come to quantitatively understand its tradeoffs between accuracy and complexity.

Appendix B. Frozen particle vs. frozen center of mass

The easiest way to eliminate the d trivial translational degrees of freedom is to freeze one of the particles, say the first one, $\Delta\mathbf{R}_1 = \mathbf{0}$, which simply amounts to deleting the d rows of the rigidity matrix corresponding to that particle. Another method is to freeze the center of mass, $\sum_{i=1}^{N}\Delta\mathbf{R}_i = \mathbf{0}$, which amounts to adding d columns to the rigidity matrix. When performing MD in the NVT ensamble, the center of mass is frozen by virtue of momentum conservation. However, it is also possible to freeze a particle, so that collisions with it no longer conserve momentum.

The two different boundary conditions do not give the same free energy. However, the difference can be readily calculated. When one particle is frozen the natural set of independent coordinates are the displacements of the other $N-1$ particles (coordinate system F). When the center of mass is frozen we can choose the same set of independent coordinates since the displacement of the frozen particle is just the negative sum of the other displacements (coordinate system CM). The transformation between these two coordinate systems is

$$\Delta\mathbf{R}^{\mathrm{CM}} = \Delta\mathbf{R}^{\mathrm{F}} - \frac{1}{N}\sum_{i=2}^{N-1}\Delta\mathbf{R}_i^{\mathrm{F}} = \mathbf{J}\Delta\mathbf{R}^{\mathrm{F}},$$

where the Jacobian $\mathbf{J} = \mathbf{I} - \Delta\mathbf{J}$ and $\Delta\mathbf{J}$ is a block matrix made up of $d \times d$ diagonal blocks which have $-1/N$ on the diagonal. The determinant of this Jacobian can be calculated to be

$$|\mathbf{J}| = \frac{1}{N^d},$$

which relates the ratios of configurational volumes in the two different coordinate systems. For the free energy per particle we thus have the transformation

$$f^{\mathrm{CM}} = f^{\mathrm{F}} - \frac{\mathrm{d}\ln N}{N},$$

the difference of course vanishing in the infinite system limit. A term of the order $\ln N/N$ is the leading finite-size correction in other free-energy methods as well [26].

Appendix C. The free energy of an ellipse in a cell

In this Appendix we consider analytic expressions for the free energy of an ellipse of aspect ratio α enclosed in a fixed cell that is of the same shape but $1+\Delta\mu$ times larger, in the limit of small $\Delta\mu$. In this limit we can linearize the non-overlap condition between the inner and outer ellipses. However, unlike the case of two disjoint ellipsoids, there is no unique contact point around which to linearize the non-overlap. Instead, every point on the ellipse is a potential contact point, and therefore the linearization of the non-overlap condition consists of infinitely many linear inequalities. For a given potential contact $\mathbf{r}_{\mathrm{C}}$ on the ellipse with a (normalized) normal vector $\mathbf{n}$, the linearized non-overlap condition is

$$\mathbf{n}^{\mathrm{T}}(\Delta\mathbf{r} + \Delta\boldsymbol{\varphi} \times \mathbf{r}_{\mathrm{C}}) \leqslant \Delta l = \Delta\mu(\mathbf{n}^{\mathrm{T}}\mathbf{r}_{\mathrm{C}}), \tag{C1}$$

where $\Delta\mathbf{r}$ and $\Delta\boldsymbol{\varphi}$ are the translational and orientational displacement of the ellipse, and Δl is the gap between the "surfaces" of the inner and outer ellipse. Since the ellipse is a smooth convex shape the mapping between $\mathbf{n}$ and $\mathbf{r}_{\mathrm{C}}$ is unique [9],

$$\mathbf{r}_{\mathrm{C}} = \frac{\mathbf{X}^{-1}\mathbf{n}}{\sqrt{\mathbf{n}^{\mathrm{T}}\mathbf{X}^{-1}\mathbf{n}}},$$

where $\mathbf{X} = \mathrm{Diag}\{1, \alpha^{-2}\}$. The three dimensional convex set of allowed displacements of the inner ellipse $\mathscr{J}_{\Delta\mathbf{q}}$ is bounded by the infinite collection of linear inequalities in $\Delta\mathbf{q} = (\Delta\mathbf{r}, \Delta\boldsymbol{\varphi})$ as given by Eq. (C1), for all $\mathbf{n} = (\cos\theta, \sin\theta)$. We are interested in calculating its volume. It is clear that its extents scale linearly with $\Delta\mu$, and its volume is therefore $V(\Delta\mu) = \Delta\mu^3 V(\Delta\mu = 1)$. We can thus focus on the case $\Delta\mu = 1$.

It is not trivial to calculate the volume $V(\mathscr{J}_{\Delta\mathbf{q}})$. We approached the problem by considering a fixed $\Delta\phi$ and then attempting to find an analytic representation of the resulting planar set of feasible $\Delta\mathbf{r}$, $\mathscr{J}_{\Delta\mathbf{r}}$, so that its area can be calculated. For example, for the trivial case $\Delta\phi = 0$, $\mathscr{J}_{\Delta\mathbf{r}}$ is simply an ellipse of aspect ratio α (this is easy to see geometrically). The maximum possible $\Delta\phi$ corresponds to only $\Delta\mathbf{r} = 0$ being feasible, and in the particular case $\alpha = 2$ it is $\Delta\phi_{\max} = 4/3$. Unfortunately, for sufficiently large $\Delta\phi$ the convex $\mathscr{J}_{\Delta\mathbf{r}}$ is not smooth, so that it cannot be parameterized by a continuous family of normal vectors. We therefore partially resorted to numerical calculations of the area of $\mathscr{J}_{\Delta\mathbf{r}}(\Delta\phi)$, and then numerically integrated

$$V = \int_{-\Delta\phi_{\max}}^{\Delta\phi_{\max}} \mathscr{J}_{\Delta\mathbf{r}} \mathrm{d}(\Delta\phi).$$

For the particular case of an ellipse with semiaxes 1 and 2 we obtained the final result

$$f_c = -2.268 - 3\ln\Delta\mu,$$

which was used in the body of this paper. It is desirable that the general case be worked out analytically, particularly for ellipsoids in three dimensions.

Appendix D. Contribution to the free energy from rattlers

Computer-generated packings often have *rattlers*, particles which do not participate in the jammed backbone of the packing and are free to rattle inside a cage formed by the jammed backbone. Near the jamming limit, systems with rattlers fall out of equilibrium on the time-scale of the BCMD algorithm because the rattlers heat up less than the other particles and the equipartition theorem no longer holds. In essence, two time-scales emerge, a short time-scale for the backbone and a long time scale for the rattlers, and the theory in Section A no longer applies. The usual "velocity-rescaling" thermostat, i.e., a uniform cooling of the whole system [9], is not appropriate since it lowers the rattler temperature more than the backbone. A better thermostat is to completely reinitialize all the particle velocities to random values as a way to cool down the system. This strategy affects the natural dynamics of the system but is necessary because the separation in time-scales between the dynamics of the rattlers and the jammed particles makes the system non-ergodic on the time-scale of the simulation.

For hard spheres in three dimensions, Eqs. (2) and (11) suggest that in the neighbourhood of the jamming point the excess free energy (relative to the ideal gas) increases with density as

$$\Delta f_J(\phi) = b\left\{-3\ln\left(1-\frac{\phi}{\phi_J}\right) - \left[\ln\left(\frac{2b\phi_J}{9\pi}\right) - 1\right] - f_J\right\} + (1-b)\Delta f_r, \tag{D1}$$

where $b \approx 1 - 0.025$ is the fraction of particles participating in the jamming backbone, and Δf_r is the contribution due to the trapping of rattlers inside the cage of jammed particles (assumed to be independent of ϕ sufficiently close to the jamming point). We can measure the rattler contribution $(1-b)\Delta f_r = r\Delta f_r$ by using the BCMD method as follows. We freeze all non-rattling particles and then perform the BCMD algorithm (in reverse) on just the rattlers, starting with bounding cells small enough so that they are disjoint with other particles, and ending with cells which are large enough so that they do not affect the rattler free volume. The resulting excess free energy for the cell-constrained rattler system, scaled by $r = 1 - b$, is shown in Fig. 5. It is seen that even though the fraction of rattlers is small, their excess free energy relative to the ideal gas is rather high (i.e., the rattler cages are rather tight) and thus the contribution to $\Delta f_J(\phi)$ is significant and cannot be neglected if one wants to calculate free energies to accuracy better than 0.1 N $k_B T$.

References

[1] J.M. Rickman, R. LeSar, Free-energy calculations in materials research, Ann. Rev. Mater. Res. 32 (2002) 195–217.
[2] L.V. Woodcock, Computation of the free energy of alternative crystal structures of hard spheres, Faraday Discuss. 106 (1997) 325–338.
[3] S.-C. Mau, D.A. Huse, Stacking entropy of hard-sphere crystals, Phys. Rev. E 59 (1999) 4396–4401.
[4] H. Koch, C. Radin, L. Sadun, Most stable structure for hard spheres, Phys. Rev. E 72 (2005) 016708.
[5] F. Sciortino, W. Kob, P. Tartaglia, Inherent structure entropy of supercooled liquids, Phys. Rev. Lett. 83 (1999) 3214–3217.
[6] S. Sastry, Evaluation of the configurational entropy of a model liquid from computer simulations, J. Phys.: Condens. Mater. 12 (29) (2000) 6515–6523.
[7] Q. Yan, T.S. Jain, J.J. de Pablo, Density-of-states Monte Carlo simulation of a binary glass, Phys. Rev. Lett. 92 (2004) 235701.
[8] L. Angelani, G. Foffi, F. Sciortino, Configurational entropy of hard spheres, arXiv:cond-mat/0506447, 2005.
[9] A. Donev, S. Torquato, F.H. Stillinger, Neighbor list collision-driven molecular dynamics simulation for nonspherical particles: I. Algorithmic details II. Applications to ellipses and ellipsoids, J. Comp. Phys 202 (2) (2005) 737–764, 765–793.
[10] A. Donev, F.H. Stillinger, S. Torquato, Do binary hard disks exhibit an ideal glass transition? Phys. Rev. Lett. 96 (22) (2006) 225502.

[11] A. Donev, F.H. Stillinger, S. Torquato, Configurational entropy of binary hard-disk glasses: nonexistence of an ideal glass transition. in preparation.
[12] R.J. Speedy, The entropy of a glass, Mol. Phys. 80 (5) (1993) 1105–1120.
[13] A. Donev, S. Torquato, F.H. Stillinger, Pair correlation function characteristics of nearly jammed disordered and ordered hard-sphere packings, Phys. Rev. E 71 (2005) 011105.
[14] A. Donev, S. Torquato, F.H. Stillinger, R. Connelly, A linear programming algorithm to test for jamming in hard-sphere packings, J. Comp. Phys. 197 (1) (2004) 139–166.
[15] R. Connelly, Rigidity and energy, Invent. Math. 66 (1982) 11–33.
[16] Z.W. Salsburg, W.W. Wood, Equation of state of classical hard spheres at high density, J. Chem. Phys. 37 (1962) 798.
[17] F.H. Stillinger, Z.W. Salsburg, Limiting polytope geometry for rigid rods, disks, and spheres, J. Stat. Phys. 1 (1) (1969) 179.
[18] M. Simonovits, How to compute the volume in high dimensions, Math. Program. Ser. B 97 (2003) 337–374.
[19] B. Bueler, A. Enge, K. Fukuda, Polytopes-Combinatorics and Computation, Birhauser Verlag, Basel, 2000 (Chapter Exact volume computation for polytopes: A practical study).
[20] A. Donev, Jammed packings of hard particles. PhD thesis, Princeton University, Princeton, NJ, 2006. Available from http://cherrypit.princeton.edu/donev.
[21] A. Donev, I. Cisse, D. Sachs, E.A. Variano, F.H. Stillinger, R. Connelly, S. Torquato, P.M. Chaikin, Improving the density of jammed disordered packings using ellipsoids, Science 303 (2004) 990–993.
[22] R. Connelly, W. Whiteley, Second-order rigidity and prestress stability for tensegrity frameworks, SIAM J. Discr. Math. 9 (3) (1996) 453–491.
[23] D. Frenkel, A.J.C. Ladd, New Monte Carlo method to compute the free energy of arbitrary solids. Application to the fcc and hcp phases of hard spheres, J. Chem. Phys. 81 (1984) 3188–3193, October.
[24] A.D. Bruce, A.N. Jackson, G.J. Ackland, N.B. Wilding, Lattice-switch Monte Carlo method, Phys. Rev. E 61 (2000) 906.
[25] B.D. Lubachevsky, F.H. Stillinger, Geometric properties of random disk packings, J. Stat. Phys. 60 (1990) 561–583.
[26] J.M. Polson, E. Trizac, S. Pronk, D. Frenkel, Finite-size corrections to the free energies of crystalline solids, J. Chem. Phys. 112 (2000) 5339–5342.
[27] N.F. Carnahan, K.E. Starling, Equation of state for nonattracting rigid spheres, J. Chem. Phys. 51 (1969) 635–636.
[28] W.G. Hoover, F.H. Ree, Melting transition and communal entropy for hard spheres, J. Chem. Phys. 49 (8) (1968) 3609.
[29] R.J. Speedy, Pressure and entropy of hard-sphere crystals, J. Phys. Condens. Mater. 10 (1998) 4387–4391.
[30] S. Pronk, D. Frenkel, Large difference in the elastic properties of fcc and hcp hard-sphere crystals, Phys. Rev. Lett. 90 (2003) 255501.
[31] N. Simányi, Encyclopedia of Mathematical Sciences, Mathematical Physics II, vol. 101, chapter Hard Ball Systems and Semi-Dispersive Billiards, Springer Verlag, 2000, pp. 51–88.
[32] L. Lovasz, S. Vempala, Simulated Annealing in Convex Bodies and an $O(n^4)$ Volume Algorithm, MSR-TR 2003-31, Microsoft Research, 2003.